

# We are IntechOpen, the world's leading publisher of Open Access books Built by scientists, for scientists

6,900

Open access books available

186,000

International authors and editors

200M

Downloads

Our authors are among the

154

Countries delivered to

TOP 1%

most cited scientists

12.2%

Contributors from top 500 universities



WEB OF SCIENCE™

Selection of our books indexed in the Book Citation Index  
in Web of Science™ Core Collection (BKCI)

Interested in publishing with us?  
Contact [book.department@intechopen.com](mailto:book.department@intechopen.com)

Numbers displayed above are based on latest data collected.  
For more information visit [www.intechopen.com](http://www.intechopen.com)



## ICA-Based Fetal Monitoring

Rubén Martín-Clemente and José Luis Camargo-Olivares  
University of Seville  
Spain

### 1. Introduction

Independent Component Analysis (ICA) has numerous applications in biomedical data processing (James & Hesse, 2005; Nait-Ali, 2009; Tanskanen & Viik, 2012). For example, in the last decade lots of contributions have been made in the field of EEG/MEG<sup>1</sup> analysis (artifact detection and removal, analysis of event-related brain responses, ... see e.g. Zarzoso (2009), and the references therein, for a more detailed information). More recently, several researchers have oriented their efforts towards developing ICA-based approaches to the interpretation of the electrocardiogram (ECG) and the information that can be derived from it (Castells et al., 2007). For example, Vetter *et al* (Vetter et al., 2000) have shown the great potential of ICA in the analysis of the control of the heart by the autonomic nervous system. Arrhythmia detection and, in particular, atrial fibrillation, also constitute possible applications, and several successful examples can be found in the literature (Llinares & Igual, 2009; Rieta et al., 2004).

A particularly appealing problem in tococardiography is that of applying ICA-based methods to the extraction of the fetal ECG (fECG) from maternal cutaneous potential measurements. The present clinic standard procedure for recording the fECG consists in inserting a small electrode into the mother's vagina, through the cervix, and directly under the skin of the fetus's scalp (Symonds et al., 2001). The major shortcoming of this technique is its invasiveness. The placement of the fetal scalp electrode presents certain risks to fetal safety, and cases where the mother is infected have been reported as well. Last but not least, this procedure is not suitable for use during all stages of pregnancy, and can only be performed under limited clinical circumstances: e.g. measuring the fECG with a scalp electrode is only possible during labor, as requires a dilated cervix and the rupture of the amniotic membranes. Due to these and other inconveniences, the scalp electrode is almost exclusively reserved for high risk births.

There exists, by contrast, an increasing interest in non-invasive fECG recording techniques (Hasan et al., 2009). These techniques should enable monitoring in stages of pregnancy earlier than labor, i.e. when the membranes protecting the fetus are not broken (*ante partum*), as well as being comfortable to women, while avoiding the risks of infection or trauma to the fetal scalp. A method for non-invasive fECG monitoring measures the fECG by means of surface electrodes placed on the mother's abdomen. It turns out that the electrical signals recorded

---

<sup>1</sup> EEG and MEG are abbreviations for, respectively, electro-encephalography and magneto-encephalography.

by the electrodes are a mixture of several electrophysiological signals and noise. Examples of the former are the maternal electrocardiogram (mECG), the electrohysterogram (EHG, the electrical activity of the uterus) and the fECG. The EHG usually lies below 3 Hz and can be reduced significantly by the use of a simple high-pass filter (Devedeux et al., 1993). The main source of noise is the power line signal (50 – 60 Hz, depending on your country), that can be eliminated by a notch filter. The limiting factor in non-invasive fetal electrocardiography is the low amplitude of the fetal electrocardiogram compared to the mECG<sup>2</sup>. As there is a considerable overlap between the frequency bands of the mECG and the fECG (Abboud & Sadeh, 1989), the mECG cannot be suppressed by a simple linear filter. A variety of different approaches have been proposed to extract the fECG from abdominal recordings (Hasan et al., 2009). In this Chapter, we describe and illustrate the specific application of ICA to this exciting problem. Potential readers are assumed very familiar with ICA —if not, they are directed to the classical textbooks Cichocki & Amari (2002); Comon & Jutten (2010); Hyvärinen et al. (2001). The Chapter is organized as follows: in Section 2, we introduce some basic concepts of fetal electrocardiography. Sections 3 and 4 discuss a simple mathematical model of the fECG and its implications for ICA. In Section 5, we review some ICA-based approaches for the fECG extraction problem. Rather than surveying superficially several methods, we shall concentrate on some of the more conceptually appealing concepts. Section 6 introduces a recent and powerful approach, namely to use the mECG as reference for the ICA algorithms. Experiments, using real data, are presented in Section 7. Finally, Section 8 is devoted to the Conclusions.

## 2. Basic background in cardiac physiology

The heart consist of four chambers: the right and left atrium and the right and left ventricle.

- In the **adult**, the atria are collecting chambers that receive the blood from the body and lungs, whereas the ventricles act as pumping chambers that send out the blood to the body tissues and lungs. Blood circulates as follows (Guyton & Hall, 1996):
  1. Oxygen-depleted blood flows into the right atrium from the body, via the vena cava.
  2. From the right atrium the blood passes into the right ventricle.
  3. The right ventricle pumps the blood, through the pulmonary arteries, into the lungs, where carbon dioxide is exchanged for oxygen.
  4. The oxygenated blood returns to the heart, via the pulmonary vein, into the left atrium.
  5. From the left atrium the blood passes into the left ventricle.
  6. The left ventricle pumps the oxygenated blood into all parts of the body through the aorta artery, and the cycle begins again.
- In the **fetus**, things are slightly different. The fetus receives the oxygen across the placenta and, as a consequence, does not use its lungs until birth. To prevent the blood to be pumped to the lungs, the pulmonary artery is connected to the aorta by a blood vessel called the arterial duct (*ductus arteriosus*). Thus, after the right ventricle contraction, most blood flows through the duct to the aorta. The fetal heart also has an opening between the right and left atria called the *foramen ovale*. The foramen ovale allows oxygenated blood

---

<sup>2</sup> Whereas the mECG shows an amplitude of up to 10 mV, the fECG often does not reach more than 1  $\mu$ V.

to flow from the right atrium to the left atrium, where it gets pumped around the body, again avoiding the lungs. Both the ductus arteriosus and the foramen ovale disappear after birth over the course of a few days or weeks (Abuhamad & Chaoui, 2009).

## 2.1 The fECG

The electrocardiogram (ECG) reflects the electrical activity of the heart as seen from the body surface. The heart generates electrical currents that radiate on all directions and result in electrical potentials. The potential difference between a pair of electrodes placed in predefined points of the surface of the body (*cutaneous recordings*), visualized as a function of time, is what we call the ECG.

The fetal electrocardiogram (fECG), like that of the adult, consists of a P wave, a QRS complex and a T wave, separated by the PR and ST intervals (see Fig. 1) (Symonds et al., 2001). These waves represent the summation of the electrical potentials within the heart. Contraction (depolarization) of both atria begins at about the middle of the P wave and continues during the PR segment. The QRS complex precedes ventricular contraction: pumping of blood normally begins at the end of the QRS complex and continues to the end of the T wave. Finally, the T wave corresponds to the electrical activity produced when the ventricles are recharging for the next contraction (repolarizing)<sup>3</sup>. Note that the repolarization of the atria is too weak to be detected on the ECG. The fECG cannot be usually detected between 28 and 32 weeks (sometimes 34 weeks) of gestation due to the isolating effect of the *vernix caseosa*, a sebum that protects the skin of the fetus (Oostendorp et al., 1989a).

The fECG provides useful information about the health and the condition of the fetus (Pardi et al., 1986): for example, the duration of the ST-segment is important in the diagnosis of fetal hypoxia (i.e. a continued lack of oxygen), and it has been also shown that both the QT interval and T-wave changes are predictive of fetal acidemia (Jenkins et al., 2005). The human heart begins beating at around 21 days after conception with frequency about 65 beats per minute (bpm). This frequency increases during the gestation up to 110 – 160 bpm before delivery. When it is not within this range, it may be indicative of serious potential health issues: e.g. if the fetal heart rate (FHR) is below 110 bpm for 10 minutes or longer (bradycardia), it is considered a *late* sign of hypoxia (there is a depression of the heart activity caused by the lack of oxygen), and a fetal emergency (Freeman & Garite, 2003). On the contrary, an FHR that exceeds 160 bpm (tachycardia) may be an *early* sign of hypoxia (other conditions that increase the FHR include fetal infection, maternal dehydration, medication, et cetera) (Afriat & Kopel, 2008).

## 3. Mathematical model of the ECG

In the **adult**, the cardiac surface potentials can be approximately considered as originated from a current dipole located in the heart (Symonds et al., 2001). Assuming that the body is a volume conductor, homogeneous and infinite, the potential due to a dipole of moment  $\mathbf{p}(t)$  at a point on the skin specified by the position vector  $\mathbf{r}$  is given by (Keener & Sneyd, 2009):

<sup>3</sup> Both atria contract and pump the blood together. Both ventricles also contract together. But the atria contract before the ventricles. Nevertheless, all the four chambers relax (stop pushing in) together.

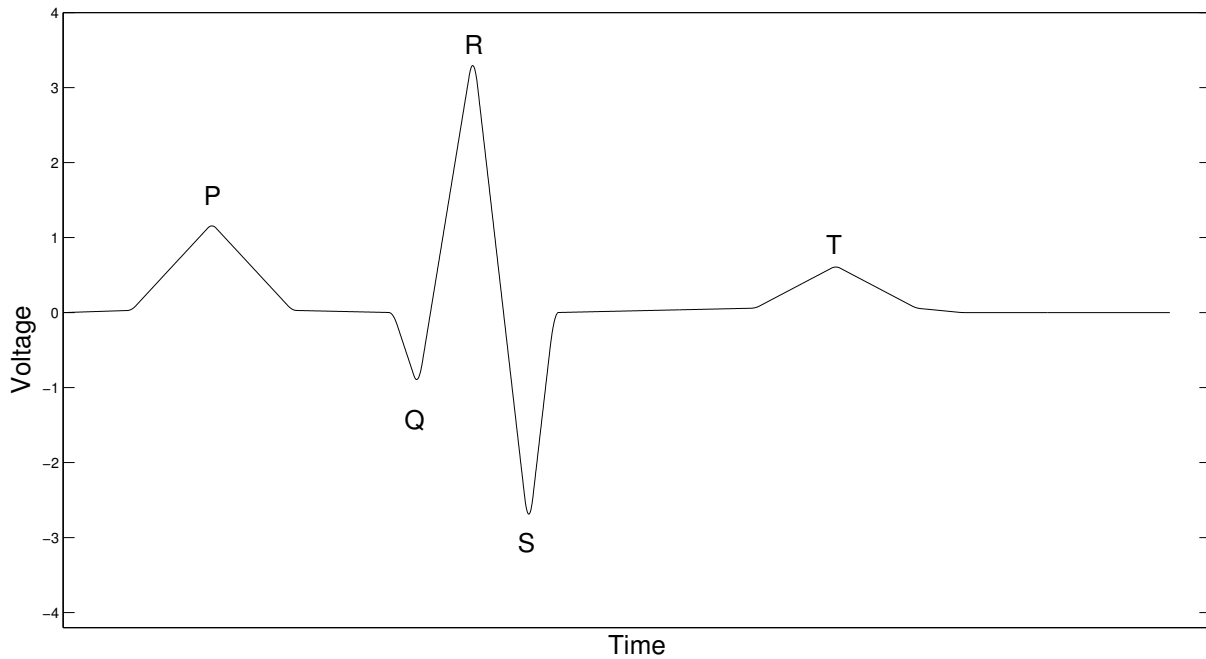


Fig. 1. Sketch of a typical single ECG recording. Note that the actual size and polarity of each wave depend on the location of the recording electrodes (Chan, 2008; Keener & Sneyd, 2009).

$$v(t) = \mathbf{p}(t) \frac{\mathbf{r}}{4\pi\sigma |\mathbf{r}|^3} \quad (1)$$

where  $\sigma$  is the permittivity of the medium. Let  $\mathbf{e}_1, \mathbf{e}_2, \mathbf{e}_3$  be orthonormal basis vectors in the real three-dimensional space and let  $\{s_1(t), s_2(t), s_3(t)\}$  be the coordinates of  $\mathbf{p}(t)$  in this basis, i.e.,

$$\mathbf{p}(t) = \sum_{i=1}^3 s_i(t) \mathbf{e}_i.$$

The body surface potential at  $\mathbf{r}$  can be then written as linear combination of the signals  $s_i(t)$ :

$$v(t) = \sum_{i=1}^3 a_i s_i(t), \quad (2)$$

where:

$$a_i \stackrel{def}{=} \mathbf{e}_i \frac{\mathbf{r}}{4\pi\sigma |\mathbf{r}|^3}.$$

It is quite noteworthy that  $\mathbf{p}(t)$  is allowed to change in orientation and strength as a function of time. For the reference of the reader, the tip of the vector traces out a loop in the space that is called *vectorcardiogram* (VCG) (Symonds et al., 2001). Different models for  $\mathbf{p}(t)$  can be found in the literature. For example, Sameni, Clifford, Jutten & Shamsollahi (2007), based on McSharry et al. (2003)<sup>4</sup>, have proposed the following differential equations for the dipole vector:

<sup>4</sup> In essence, McSharry et al. (2003) describe each wave of the ECG (P, Q, R, S and T) by a Gaussian function whose amplitude, width and temporal location have to be determined.

$$\begin{aligned}
\dot{\vartheta} &= \omega, \\
\dot{s}_1 &= - \sum_i \frac{\alpha_i^1 \omega}{(b_i^1)^2} \Delta\vartheta_i^1 \exp \left[ - \frac{(\Delta\vartheta_i^1)^2}{2(b_i^1)^2} \right], \\
\dot{s}_2 &= - \sum_i \frac{\alpha_i^2 \omega}{(b_i^2)^2} \Delta\vartheta_i^2 \exp \left[ - \frac{(\Delta\vartheta_i^2)^2}{2(b_i^2)^2} \right], \\
\dot{s}_3 &= - \sum_i \frac{\alpha_i^3 \omega}{(b_i^3)^2} \Delta\vartheta_i^3 \exp \left[ - \frac{(\Delta\vartheta_i^3)^2}{2(b_i^3)^2} \right],
\end{aligned} \tag{3}$$

where  $\Delta\vartheta_i^1 = (\vartheta - \vartheta_i^1) \bmod(2\pi)$ ,  $\Delta\vartheta_i^2 = (\vartheta - \vartheta_i^2) \bmod(2\pi)$ ,  $\Delta\vartheta_i^3 = (\vartheta - \vartheta_i^3) \bmod(2\pi)$  and  $\omega = 2\pi f$ , where  $f$  is the beat-to-beat rate. Note also that the equation  $\dot{\vartheta} = \omega$  generates periodic signals with the frequency of the heart rate. The problem of estimating the parameters  $\alpha_i^k, b_i^k, \vartheta_i^k$  of the model is complicated and has been addressed, e.g., in (Clifford et al., 2005; Sameni, Shamsollahi, Jutten & Clifford, 2007).

### 3.1 The fECG case

Is the previous dipole-based model capable of describing the potential distribution created by the fetal heart at the maternal abdomen? It depends. At early pregnancies, from week 20 until 28 of gestation, the amplitude of the fECG increases and the model seems to be appropriate and fits the observations well (Oostendorp et al., 1989a). Late in pregnancy, however, great care is needed: we have already mentioned that the fECG is in general impossible to measure between 28th to 32th week of gestation due to the isolating effect of the *vernix caseosa*, the fatty layer that protects the skin of the fetus (Wakai et al., 2000). After the 32th week, the fECG is detected again, but the apparent fetal vectorcardiogram (fVCG), as calculated from the recorded surface potentials, describes almost a straight line (Oldenburg & Macklin, 1977). Hence it no longer corresponds to the activity of the fetal heart vector in an intelligible way. It has been hypothesized that, as the fetus grows, several holes appear in the vernix<sup>5</sup> and current can escape through them (Peters et al., 2005). It turns out that the potential is split up into a contribution of the current dipole and a contribution of the volume currents induced in the vernix. Experiments confirm that, after the 32th week, the fECG recorded at the mother's abdomen can be still described by a model of the type (2), i.e.,

$$v(t) = \sum_{i=1}^n a_i s_i(t), \tag{4}$$

but the fetal source signals  $s_i(t)$  cannot be longer interpretable as coordinates of a single current dipole. Rather, we should think of eqn. (4) more as a *latent variable model*. Note that, by definition, the latent variables  $s_i(t)$  correspond to abstract or hypothetical concepts. Experiments also show that the number of summands  $n$  may be different (usually less) from three (Oostendorp et al., 1989b; Sameni, Clifford, Jutten & Shamsollahi, 2007). See also (Lewis, 2003) and the references therein.

<sup>5</sup> The most important hole is probably at the mouth. A second relevant hole can be expected at the base of the umbilical cord.

#### 4. ICA model

Thus, in view of the previous Section, ECGs seem to satisfy some of the conditions for classical ICA:

- The body surface potentials are a linear mixture of several source signals.
- Time delays in signal transmission are negligible.
- It is feasible to have more observations than sources<sup>6</sup>.

Let  $v_1(t), \dots, v_p(t)$  be *zero-mean* signals recorded from electrodes placed on the mother's body, where  $t \in \mathbb{Z}$  is the discrete time. Each measurement signal  $v_i(t)$  is modelled as a linear combination of  $r$  ( $r \leq 6$ ) bioelectric source signals, that have similar definitions to the ones in eqns. (2)–(4), plus noise:

$$\begin{aligned} v_1(t) &= a_{11} s_1(t) + \dots + a_{1r} s_r(t) + n_1(t) \\ &\vdots \\ v_p(t) &= a_{p1} s_1(t) + \dots + a_{pr} s_r(t) + n_p(t) \end{aligned} \quad (5)$$

The noise represents the signal degradation due, for example, to baseline wander, mains interference, uterine contractions, and so on. Eqn. (5) can be rewritten in matrix form as:

$$\mathbf{v}(t) = \mathbf{A} \mathbf{s}(t) + \mathbf{n}(t) \quad (6)$$

where  $\mathbf{v}(t)$  be the vector whose  $i$ th component is  $v_i(t)$  and so on. Eqn. (5) represents the superposition of the body surface potentials due to the fetus and the maternal cardiac dipole. Note that  $\mathbf{s}(t)$  can be partitioned into a block of maternal signals and a block of fetal signals, and there exists a corresponding partitioning for  $\mathbf{A}$ :

$$\mathbf{s}(t) = \begin{bmatrix} \mathbf{s}_M(t) \\ \mathbf{s}_F(t) \end{bmatrix}, \quad \mathbf{A} = [\mathbf{A}_M \mathbf{A}_F] \quad (7)$$

Thus:

$$\mathbf{v}(t) = \mathbf{A}_M \mathbf{s}_M(t) + \mathbf{A}_F \mathbf{s}_F(t) + \mathbf{n}(t) \quad (8)$$

The fetal electrocardiogram contributions to the measurement signals can then be obtained by:

$$\mathbf{v}_F(t) = \mathbf{A}_F \mathbf{s}_F(t) \quad (9)$$

Observe that (9) allows the estimation of the fetal electrocardiogram contributions to *all* leads. Similarly, the mothers' own ECG is given by:

$$\mathbf{v}_M(t) = \mathbf{A}_M \mathbf{s}_M(t) \quad (10)$$

Note that  $\mathbf{v}_M(t)$  belongs to the column space of  $\mathbf{A}_M$ , which is usually renamed as the *mECG subspace*. Similarly, the column space of  $\mathbf{A}_F$  will be denoted as the *fECG subspace*. Recalling again the discussion in the previous Section, the mECG space can be assumed a three dimensional vector space. However, the dimension of the fECG space is not necessarily equal to three (three is its maximum value) and is subject to changes during the pregnancy (Sameni, Clifford, Jutten & Shamsollahi, 2007).

<sup>6</sup> According to the model, there are, at most, six cardiac bioelectric sources.

The main assumption of the ICA model, the independence between sources, leads to some confusion. Even though this assumption is usually adopted (De Lathauwer et al., 2000a), there is no evidence to support it. The source signals can be actually partitioned into groups (a maternal group and a fetal group); components from different groups are statistically independent (i.e., there is a lack of dependency between coincident source activations), but components of the same group may be dependent. This is the concept of Multidimensional Independent Component Analysis (MICA), which is closely related to Independent Subspace Analysis (ISA) (Comon & Jutten, 2010; Hyvärinen et al., 2001). The idea of MICA, originally proposed in Cardoso (1998), has been further developed in Theis (2004) and Vollgraf & Obermayer (2001) among others. MICA actually proceeds in two steps (Cardoso, 1998): firstly, it runs a traditional ICA algorithm<sup>7</sup> and, then, it is determined which outputs of the algorithm are really independent and which should be grouped together (though the latter may not be trivial). Once we have recovered the source signals, we may use them to estimate (9), i.e. the fECG part of the composite signal, depending on the desired application.

#### 4.1 Electrode placement

The number of electrodes and the positions at which these should be placed is not standardized. The situation is complex due to the fact that the fetal heart position with respect to the maternal abdomen varies with time and cannot be easily determined. Nevertheless, for late pregnancies, it has been observed that the fECG morphology is almost independent of electrode position (Lewis, 2003). A large number of electrodes (more than 30) arranged in a wide belt around the mother's abdomen, also containing some electrodes at the back, has been used in laboratory experiments (Cicinelli et al., 1994; Oostendorp, 1989; Vrins et al., 2004).

### 5. Algorithms

To the best of our knowledge, De Lathauwer *et al* were the first investigators to show that the application of MICA (Cardoso, 1998), or ISA (Comon & Jutten, 2010; Hyvärinen et al., 2001), to  $v_1(t), \dots, v_N(t)$  succeeds in the extraction of the fECG (De Lathauwer et al., 1995; 2000a). This observation has been subsequently confirmed by many other researchers (Clifford et al., 2011; Sameni et al., 2006; Zarzoso & Nandi, 2001), even in twin and triplet pregnancies (Keralapura et al., 2011; Taylor et al., 2003; 2005). In the literature, we have found numerous general-purpose ICA algorithms that solve the fECG extraction problem. For example, they include the *contrast maximization* (CoM2) method (Comon, 1994), JADE (Cardoso & Souloumiac, 1993), INFOMAX (Bell & Sejnowski, 1995), FastICA (Hyvärinen, 1999), Barros' method (Barros & Cichocki, 2001; Li & Yi, 2008), SOBI (Belouchrani et al., 1997), Pearson-ICA (Karvanen et al., 2000) or MERMAID (Marossero et al., 2003). ICA has been also used in combination with Wavelet transforms (Azzerboni et al., 2005; Vigneron et al., 2003), singular value decompositions (Gao et al., 2003) and neural networks (Yu & Chou, 2008), to cite some few examples. For a review of non-ICA based approaches, see, e.g. (Hasan et al., 2009). Naturally we cannot cover all the existing methods. Instead of surveying superficially several of them, we shall concentrate on some conceptually appealing aspects, some of which are not generally found in the literature.

<sup>7</sup> Some ICA algorithms output signals that are solutions to the MICA problem in the two-step approach described above.

### 5.1 Subspace analysis (whitening)

*Whitening* is the classical pre-processing for ICA and it is surely well-known to most of the readers of this book (otherwise, see, e.g., Comon & Jutten (2010)). For this reason, we offer an alternative viewpoint and present here whitening as a classical technique of subspace analysis. The idea is to use whitening to estimate the mECG subspace (or, more precisely, to estimate its orthogonal complement<sup>8</sup>). Then, the mECG can be easily projected out of the dataset. This approach (and its variants) has been conveniently addressed in several papers (see e.g. Callaerts et al. (1990); De Lathauwer et al. (2000b); Kanjilal et al. (1997)). We shall try to focus on the most relevant aspects: consider that we are given  $q$  samples  $\mathbf{v}(1), \dots, \mathbf{v}(q)$  of the vector signal  $\mathbf{v}(t)$ . In order to get rid of the maternal electrocardiogram interference, the eigenvalue decomposition of the data covariance matrix:

$$\mathbf{R}_v = \frac{1}{q} \sum_{t=1}^q \mathbf{v}(t) \mathbf{v}^T(t)$$

is first computed. Since  $\mathbf{R}_v$  is always symmetric and nonnegative definite, it can be factorized into  $\mathbf{R}_v = \mathbf{Q} \mathbf{D} \mathbf{Q}^T$ , where:

$$\mathbf{D} = \text{diag} (\lambda_1 \geq \lambda_2 \geq \dots \geq \lambda_p)$$

is the  $p \times p$  diagonal matrix whose elements are the eigenvalues of  $\mathbf{R}_v$  and  $\mathbf{Q}$  is the matrix containing the corresponding eigenvectors. If the maternal electrocardiogram is strong enough, it has been shown that the  $M$  largest eigenvalues in  $\mathbf{D}$  are associated with it. Furthermore, it holds that the eigenvalues have usually the following typical relationship:

$$\lambda_1 \geq \lambda_2 \geq \dots \geq \lambda_n > \lambda_{n+1} \approx \dots \approx \lambda_p.$$

This means that the last  $(p - n)$  minor eigenvalues correspond to the noise. Matrices  $\mathbf{D}$  and  $\mathbf{Q}$  can be then partitioned into three groups:

$$\mathbf{D} = \begin{pmatrix} \mathbf{D}_1 & \mathbf{0} & \mathbf{0} \\ \mathbf{0} & \mathbf{D}_2 & \mathbf{0} \\ \mathbf{0} & \mathbf{0} & \mathbf{D}_3 \end{pmatrix} \quad \mathbf{Q} = (\mathbf{Q}_1 \quad \mathbf{Q}_2 \quad \mathbf{Q}_3)$$

where  $\mathbf{D}_1$  contains those  $M$  largest eigenvalues, and the columns of  $\mathbf{Q}_1$  are the corresponding eigenvectors;  $\mathbf{D}_2 = \text{diag} (\lambda_{M+1} \dots \lambda_n)$  and  $\mathbf{Q}_2$  contains the associated eigenvectors, *et cetera*. The maternal electrocardiogram can be then eliminated by projecting the data onto the subspace spanned by  $\mathbf{Q}_2$ . Specifically, this can be written as:

$$\mathbf{z}(t) = \mathbf{Q}_2^T \mathbf{v}(t) \tag{11}$$

where  $\mathbf{z}(t)$  is the  $(p - M) \times 1$  vector that, in theory, contains *no* maternal contribution, making the identification of the fetal electrocardiogram a feasible task, even by simple inspection<sup>9</sup>. Of course, the determination of  $M$  is an important problem. Seminal works considered  $M = 3$ ; however, it has been recently argued that from  $M = 4$  to  $M = 6$  may be required in some cases. In practice, experiments suggest finding  $M$  empirically from the gap between the eigenvalues

<sup>8</sup> The orthogonal complement is the set of all vectors that are orthogonal to the vectors in the mECG space.

<sup>9</sup> In fact, under further hypotheses, it holds that  $\mathbf{s}_F(t) = \mathbf{D}_2^{-1/2} \mathbf{Q}_2^T \mathbf{v}(t)$  and  $\mathbf{A}_F = \mathbf{Q}_2 \mathbf{D}_2^{1/2}$ .

of the data covariance matrix. The complete procedure can be accomplished in real time with low computational cost. In any case, the performance of the whitening-based approaches is strongly dependent on the position of the electrodes (Callaerts et al., 1990), which usually becomes a matter of trial and error.

## 5.2 $\pi$ CA

The combination of the measured signals  $v_i(t)$  to enhance the periodic structure of the fECG also seems to be a promising idea. The algorithm should combine in power (constructive interference) the fetal components and cancel each other out (destructive interference). The best-known approach is to seek for the linear combination  $y(t) = \sum_i w_i v_i(t) = \mathbf{w}^T \mathbf{v}(t)$  that minimizes the following measure of periodicity:

$$\varepsilon(\mathbf{w}, \tau) = \frac{\sum_t |y(t + \tau) - y(t)|^2}{\sum_t y^2(t)}, \quad (12)$$

where the time-lag  $\tau$  is the period of interest (in theory, but not always in practice,  $\tau =$  the fetal period —see below). This approach has been named *Periodic Component Analysis* ( $\pi$ CA), and was first used for representing periodic structure in speech (Saul & Allen, 2001). The application of  $\pi$ CA to the fECG extraction problem can be traced back to the paper (Sameni et al., 2008). The minimization of (12) can be easily accomplished in a linear algebra framework. Expanding the right-hand side of (12) gives:

$$\begin{aligned} \varepsilon(\mathbf{w}, \tau) &= \frac{\sum_t y^2(t + \tau) + y^2(t) - 2y(t + \tau)y(t)}{\sum_t y^2(t)} \\ &= \frac{\sum_t \mathbf{w}^T \mathbf{v}(t + \tau) \mathbf{v}^T(t + \tau) \mathbf{w} + \sum_t \mathbf{w}^T \mathbf{v}(t) \mathbf{v}^T(t) \mathbf{w} - 2 \sum_t \mathbf{w}^T \mathbf{v}(t + \tau) \mathbf{v}^T(t) \mathbf{w}}{\sum_t \mathbf{w}^T \mathbf{v}(t) \mathbf{v}^T(t) \mathbf{w}} \quad (13) \\ &= 2 \left[ 1 - \frac{\mathbf{w}^T \mathbf{C}_v(\tau) \mathbf{w}}{\mathbf{w}^T \mathbf{C}_v(0) \mathbf{w}} \right], \end{aligned}$$

where  $\mathbf{C}_v(\tau)$  is the sample covariance matrix defined by:

$$\mathbf{C}_v(\tau) = \frac{1}{q} \sum_t \mathbf{v}(t + \tau) \mathbf{v}^T(t). \quad (14)$$

Now consider the whitened data:

$$\mathbf{z}(t) = \mathbf{D}_1^{-1/2} \mathbf{U}_1^T \mathbf{v}(t) \quad (15)$$

where  $\mathbf{D}_1$  and  $\mathbf{U}_1$  are the respective eigenvalue and eigenvector matrices of  $\mathbf{C}_v(0)$ , i.e.,

$$\mathbf{C}_v(0) = \mathbf{U}_1 \mathbf{D}_1 \mathbf{U}_1^T$$

Then we have:

$$\begin{aligned} \mathbf{C}_z(0) &= \mathbf{D}_1^{-1/2} \mathbf{U}_1^T \mathbf{C}_v(0) \mathbf{U}_1 \mathbf{D}_1^{-1/2} = \mathbf{I} \\ \mathbf{C}_z(\tau) &= \mathbf{D}_1^{-1/2} \mathbf{U}_1^T \mathbf{C}_v(\tau) \mathbf{U}_1 \mathbf{D}_1^{-1/2} \end{aligned} \quad (16)$$

where  $\mathbf{C}_z(\tau) = \frac{1}{q} \sum_t \mathbf{z}(t + \tau) \mathbf{z}^T(t)$ . Let us define:

$$\underline{\mathbf{w}} = \mathbf{D}_1^{1/2} \mathbf{U}_1^T \mathbf{w} \quad (17)$$

With this new vector, (13) can be rewritten as follows:

$$\varepsilon(\mathbf{w}, \tau) = 2 \left[ 1 - \frac{\mathbf{w}^T \mathbf{C}_z(\tau) \mathbf{w}}{\mathbf{w}^T \mathbf{C}_z(0) \mathbf{w}} \right] = 2 \left[ 1 - \frac{\mathbf{w}^T \mathbf{C}_z(\tau) \mathbf{w}}{\mathbf{w}^T \mathbf{w}} \right] \quad (18)$$

Then:

**Proposition 1.** *By the Rayleigh-Ritz theorem of linear algebra (Bai et al., 2000), the vector weight  $\mathbf{w}$  minimizing (18) is given by the eigenvector of the matrix  $\mathbf{C}_z(\tau)$  with the largest eigenvalue.*

Denoting this eigenvector by  $\mathbf{w}_{max}$ ,  $\pi$ CA then outputs:

$$\begin{aligned} y(t) &= \mathbf{w}_{max}^T \mathbf{z}(t) \\ &= \mathbf{w}_{max}^T \mathbf{D}_1^{-1/2} \mathbf{U}_1^T \mathbf{v}(t) \\ &= \mathbf{w}_{max}^T \mathbf{v}(t) \end{aligned} \quad (19)$$

with  $\mathbf{w}_{max}^T \stackrel{def}{=} \mathbf{w}_{max}^T \mathbf{D}_1^{-1/2} \mathbf{U}_1^T$ .

It is interesting to note that  $\pi$ CA is actually a particularization of the well-known *Algorithm for Multiple Unknown Signals Extraction* (AMUSE) (Tong et al., 1991): by assuming  $\mathbf{D}_2$  as the full diagonal eigenvalue matrix of  $\mathbf{C}_z(\tau)$ , with eigenvalues sorted in descending order, and  $\mathbf{U}_2$  being the corresponding eigenvector matrix<sup>10</sup>, one can write the eigendecomposition:

$$\mathbf{C}_z(\tau) = \mathbf{U}_2 \mathbf{D}_2 \mathbf{U}_2^T.$$

Then,  $\mathbf{y}(t) = \mathbf{U}_2^T \mathbf{z}(t)$  verifies:

$$\begin{aligned} \mathbf{C}_y(0) &= \mathbf{U}_2^T \mathbf{C}_z(0) \mathbf{U}_2 = \mathbf{U}_2^T \mathbf{U}_2 = \mathbf{I} \\ \mathbf{C}_y(\tau) &= \mathbf{U}_2^T \mathbf{C}_z(\tau) \mathbf{U}_2 = \mathbf{D}_2 \end{aligned} \quad (20)$$

with  $\mathbf{C}_y(\tau) = \frac{1}{q} \sum_t \mathbf{y}(t + \tau) \mathbf{y}(t)^T$ . Taking eqn. (16) into eqn. (20), we get that both matrices  $\mathbf{C}_v(0)$  and  $\mathbf{C}_v(\tau)$  are simultaneously diagonalized by matrix  $\mathbf{Q} = \mathbf{U}_2^T \mathbf{D}_1^{-1/2} \mathbf{U}_1^T$ :

$$\begin{aligned} \mathbf{Q} \mathbf{C}_v(0) \mathbf{Q}^T &= \mathbf{I} \\ \mathbf{Q} \mathbf{C}_v(\tau) \mathbf{Q}^T &= \mathbf{D}_2 \end{aligned} \quad (21)$$

As can be easily verified, this implies that:

$$\begin{aligned} \mathbf{C}_v(\tau) \mathbf{Q}^T &= \mathbf{C}_v(0) \mathbf{Q}^T \mathbf{D}_2 \\ \mathbf{C}_v^{-1}(0) \mathbf{C}_v(\tau) \mathbf{Q}^T &= \mathbf{Q}^T \mathbf{D}_2 \end{aligned} \quad (22)$$

i.e.  $\mathbf{D}_2$  and  $\mathbf{Q}^T$  are the eigenvalues and eigenvectors, respectively, of the matrix  $\mathbf{C}_v^{-1}(0) \mathbf{C}_v(\tau)$ . Then,  $\mathbf{Q}$  can be identified by the simultaneous diagonalization of  $\mathbf{C}_v(0)$  and  $\mathbf{C}_v(\tau)$ . This is the basic idea behind AMUSE.

<sup>10</sup>  $\mathbf{w}_{max}$  is the first column of  $\mathbf{U}_2$  and so on.

**Proposition 2.** Let  $\mathbf{v}(t) = \mathbf{A} \mathbf{s}(t)$ , where  $\mathbf{A}$  is of full column rank, and the sources  $s_i(t)$  are zero-mean WSS processes uncorrelated with each other. Let us choose any time delay  $\tau$  for which  $\mathbf{C}_v^{-1}(0) \mathbf{C}_v(\tau)$  has non-zero distinct eigenvalues. Then  $\mathbf{y}(t) = \mathbf{Q} \mathbf{v}(t)$  is an estimate of the source signals except for the usual scaling and ordering indeterminations.

This proposition readily follows from (Tong et al., 1991). For virtually any time-lag  $\tau \neq 0$ , AMUSE is able to output the (fetal and maternal) source signals. In addition, the requirement of the sources being mutually uncorrelated is much weaker than the classical ICA condition of mutual independence<sup>11</sup>. The transformation  $\mathbf{y}(t) = \mathbf{Q} \mathbf{v}(t) = [y_1(t), \dots, y_p(t)]^T$  can be also interpreted as follows:  $y_1(t)$  is the most periodic component with respect to the period of interest  $\tau$ ,  $y_p(t)$  is the least periodic, and the intermediate components are ranked in descending order of periodicity (Sameni et al., 2008). Of course, this does not mean that, in particular,  $y_1(t)$  is (even approximately) periodic with period  $\tau$ , neither does it mean that  $y_1(t)$  has physical meaning. Both questions depend on the specific choice of  $\tau$ .

### 5.2.1 Period calculation

No specific strategy for selecting  $\tau$  was provided in (Tong et al., 1991). A natural approach in our context is to set  $\tau$  to the value of the fetal heart beat period (which, for simplicity, is assumed to be an integer multiple of the sampling interval). However, such an approach is difficult to implement in practice, since the fetal heart beat period has to be estimated on-line, which requires the prior extraction of the fetal R peaks.

As an alternative, (Sameni et al., 2008) reports good results when  $\tau$  is chosen as the maternal ECG period. In this way, the most periodic components span the mECG subspace. In addition, see (20), the periodic components  $y_1(t), \dots, y_p(t)$  happen to be uncorrelated with each other. Hence, the space spanned by the less periodic components is orthogonal to the mECG subspace. It follows that this method is similar in spirit to the whitening-based approaches described in the previous Section.

A more challenging problem arises from the fact that the heart beat period is actually *time-dependent*. Hence, the period has to be updated on a beat-to-beat basis (see Sameni et al. (2008) for a possible solution).

### 5.2.2 Extensions

AMUSE (and, subsequently,  $\pi$ CA) suffers from the limitation that the choice of  $\tau$  is very critical. To overcome this drawback, one powerful approach is to perform the simultaneous diagonalization of more covariance matrices than just two, as is the case with AMUSE. For example, SOBI (Belouchrani et al., 1997) seeks the matrix  $\mathbf{Q}$  as the joint diagonalizer of a set of covariance matrix  $\mathbf{C}_v(\tau_i)$  for a preselected set of time-lags  $\{\tau_1, \tau_2, \tau_3, \dots\}$ . Some steps to investigate the optimal choice of  $\{\tau_1, \tau_2, \tau_3, \dots\}$  in context of the fECG extraction problem have been done by (Tsalaila et al., 2009).

### 5.3 HOS-based approach

It is well-known that, implicitly or explicitly, most ICA methods actually rely on higher-order statistics (HOS) (Comon & Jutten, 2010). Let us briefly review one of the simplest approaches:

<sup>11</sup> Correlation can be always removed by an orthogonal transformation, i.e., a change of basis in 3D space.

the maximization of the kurtosis (Hyvärinen et al., 2001). Let  $\mathbf{z}(1), \dots, \mathbf{z}(q)$  be the whitened data. Given an arbitrary vector  $\mathbf{w}$ , it follows from the central limit theorem that

$$y(t) = \mathbf{w}^T \mathbf{z}(t) \quad (23)$$

is more Gaussian when it is a sum of the fECG and the interferences than when it is equal to only one of them<sup>12</sup>. In consequence, to find  $\mathbf{w}$  in such a way that the distribution of  $y(t)$  is as far as possible from Gaussian seems to be a sound idea. This general approach to the problem of ‘unmixing’ mixed signals very common in ICA and is usually referred to as *maximisation of non-Gaussianity* (Hyvärinen et al., 2001). The simplest measure of non-Gaussianity is the kurtosis, defined by:

$$\kappa_y = \frac{1}{q} \sum_{t=1}^q y^4(t) - \frac{3}{q} \sum_{t=1}^q y^2(t) \quad (24)$$

We maximise the kurtosis of  $y(t)$  under the unit-power constraint

$$\frac{1}{q} \sum_{t=1}^q y^2(t) = 1 \quad (25)$$

which avoids the solution  $y(t) \rightarrow \infty$ . It is easily shown that this is equivalent to constraining the norm of  $\mathbf{w}$  to be the unity. Traditional ICA algorithms, such as FastICA (Hyvärinen, 1999), maximize the kurtosis using standard procedures. As an alternative, we review here the FFD (Fast Fetal Detection) method (Martín-Clemente et al., 2011) which, paradoxically, does not require to compute HOS. Consider first the following theorem, whose proof is straightforward:

**Theorem 1.** *Let  $\{x(t), t = 1, \dots, q\}$  be the samples of a generic discrete-time signal. The kurtosis of  $x(t)$ , defined by*

$$\kappa_x = \frac{1}{q} \sum_{t=1}^q x^4(t) - \frac{3}{q} \sum_{t=1}^q x^2(t)$$

*is maximized under the unit-power constraint  $\frac{1}{q} \sum_{t=1}^q x^2(t) = 1$  by signals of the form*

$$x_*(t) = \pm \sqrt{q} e_k(t)$$

*where  $e_k(t)$  is a discrete-time signal that equals one at  $t = k$  and is zero elsewhere.*

To explore the vicinity of the maximum  $\sqrt{q} e_k(t)$ , where  $k \in \{1, \dots, q\}$ , we perform a first order Taylor expansion of the kurtosis around this point (see Martín-Clemente et al. (2011) for the details):

$$\kappa_y \approx q - 3 - 2 \sum_{t=1}^q (y(t) - \sqrt{q} e_k(t))^2 \quad (26)$$

Hence  $\kappa_y$  is maximized when

$$\sum_{t=1}^q (y(t) - \sqrt{q} e_k(t))^2 \quad (27)$$

is minimum: i.e., the optimum  $y(t)$  is the signal that is as close as possible to  $\sqrt{q} e_k(t)$ . To determine the best value for the time index  $k$ , note that the accuracy of (26) increases as (27)

<sup>12</sup> The fECG can be assumed independent from the others as it has a different physical origin.

decreases. Consequently, we minimize (27) among all possible values of  $k$ . Taking into account that  $y(t) = \mathbf{w}^T \mathbf{z}(t)$ , a bit of algebra shows that the minimum is obtained simply by setting

$$\mathbf{w}_* = \frac{\mathbf{z}(K)}{\|\mathbf{z}(K)\|}, \text{ where } K = \underset{k}{\operatorname{argmax}} \|\mathbf{z}(k)\| \quad (28)$$

Consider the following additional interpretation: by construction,  $y(t)$  is the signal that is as close as possible to the impulse signal  $\sqrt{q} e_K(t)$ . If  $\mathbf{z}(t)$  is periodic, one can prove easily that  $y(t)$  is also the best approximation to an impulse train having the same period and centered upon  $t = K$ . The ECG resembles an impulse train, but the interferences degrade the measurements. The algorithm restores this property and, as result, restores the signal itself. The method may be then considered as a particular application of the class of waveform-preserving methods for recovering ECG signals.

Finally, to extract sequentially more signals, we can use the procedure described in Chapter 4 of (Cichocki & Amari, 2002). Basically, we remove  $y(t)$  from the mixture by  $\mathbf{z}'(t) = \mathbf{z}(t) - \mathbf{w} y(t)$ . Then whitening is applied again to reduce the dimensionality in one unit. The algorithm is repeated until all the desired signals are recovered.

## 6. The mECG as reference

Incorporating prior information into ICA may reduce the computational cost while improving the performance of the algorithms. The use of a reference signal has been proposed in Adib & Aboutajdine (2005), using an approach similar to that in Martín-Clemente et al. (2004). To get such a reference, ICA is often applied to data sets that include mECG signals taken at the mother's thoracic region. In this Section, we describe the variant proposed in Camargo-Olivares et al. (2011). The architecture of the proposed system is shown in Figure 2 and each block is described separately next:

1. Pre-processing block: it aims to remove the baseline wander, the electromyographic (EMG) noise, and the power line interference from each signal  $v_i(t)$ . This is usual in most contemporary ECG processing systems.
2. mECG recording: in most previous approaches, the mECG is measured at the chest of the mother. By contrast, in this paper we propose recovering the mECG directly from the mother's abdomen. We face a problem of recovering a signal (the mECG) corrupted by 'noise' (the fECG and others) at, fortunately, a very high signal-to-noise ratio. A state-of-the-art solution is that proposed in Sameni, Shamsollahi, Jutten & Clifford (2007). This filter actually *generates a synthetic* mECG whose morphology and parameters (R-R interval and so on) are calculated from the filter input. The proposed procedure is hence as follows: 1.) Filter each signal taken at the mother's abdomen by the filter described in Sameni, Shamsollahi, Jutten & Clifford (2007). 2.) Perform a linear mapping of the filter outputs to a lower dimensional space using whitening to reduce the number of mECG signals under consideration.
3. ICA block: the inputs to ICA are the pre-processed abdominal maternal signals and the mECG estimates (outputs of block 2).
4. Post-processing block: (optional) the fECG is filtered again with the filter described in Sameni, Shamsollahi, Jutten & Clifford (2007) to improve the final signal to noise ratio.

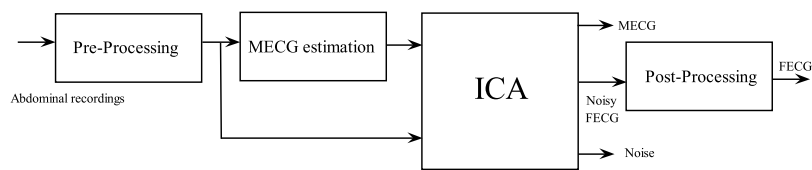


Fig. 2. Block diagram of the proposed system.

## 7. Examples

### 7.1 First example

Eight real cutaneous potential recordings of a pregnant woman were obtained from the Database for the Identification of Systems (DaISy)<sup>13</sup>. The data, see Fig. 3, consist of eight channels of ECG signals: the first five channels correspond to electrodes placed on the woman's abdominal region. The last three signals correspond to electrodes located on the mother's region. For many years, these recordings have been extensively used as the standard test data of fECG extraction algorithms (e.g., see Zarzoso & Nandi (2001)). Even though the

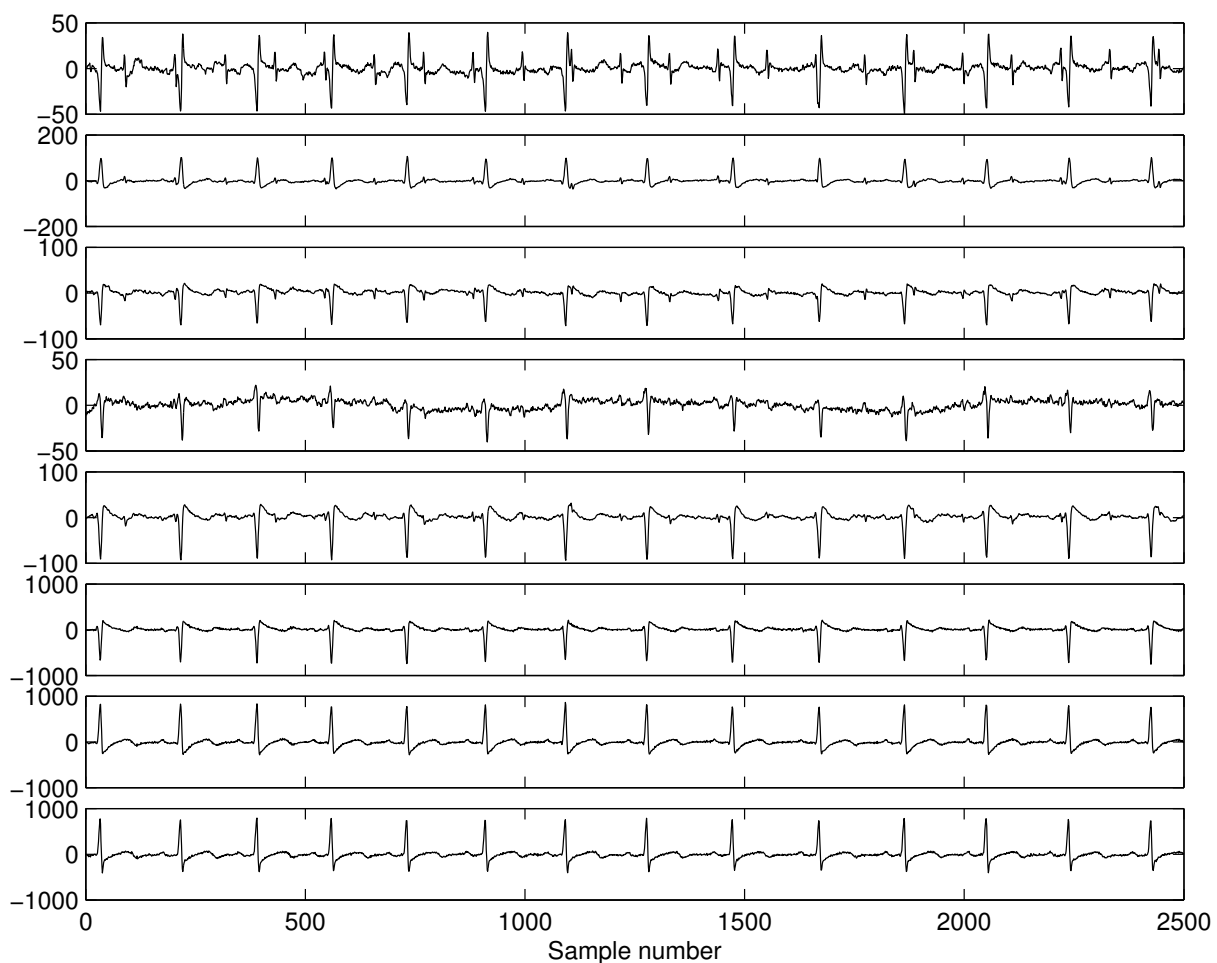


Fig. 3. Cutaneous electrode recordings from a pregnant woman.

<sup>13</sup> <ftp://ftp.esat.kuleuven.be/pub/SISTA/data/biomedical/>

fECG is much weaker than the mECG, it is slightly visible in the abdominal recordings. We applied the following ICA algorithms to these data: JADE (Cardoso & Souloumiac, 1993), FastICA (Hyvärinen, 1999), FFD (Martín-Clemente et al., 2011), SOBI (Belouchrani et al., 1997) and  $\pi$ CA (Sameni et al., 2008). Apart from whitening, no other pre-processing is used.

All the algorithms succeeded in estimating two fetal source signals. Fig. 4 shows the first one of them, as recovered by each algorithm. All methods produced very similar results. Note that the R wave is perfectly visible, allowing the easy calculation of the fetal heart rate.

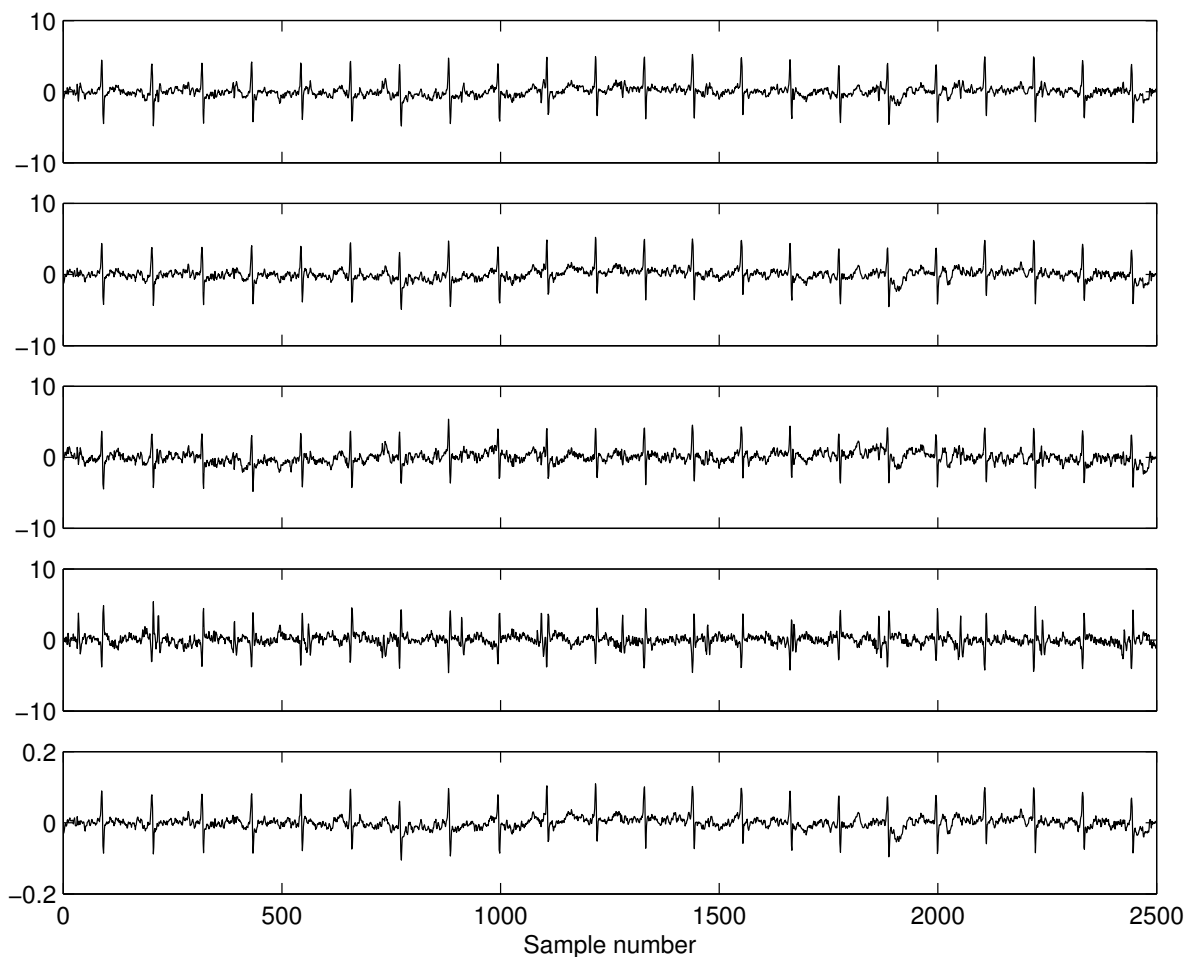


Fig. 4. Fetal source signals detected from the recordings of Fig. 3 by, from the top to the bottom, JADE, FastICA, FFD, SOBI and  $\pi$ CA.

## 7.2 Second example

The methods are now tested using experimental data from the Non-invasive Fetal Electrocardiogram database<sup>14</sup>. This public database contains a series of 55 multichannel thoracic and abdominal non-invasive recordings, taken from a single pregnant woman between 21 and 40 weeks of pregnancy. The ones used in this experiment correspond to the 21 week of gestation and are shown in Fig. 5. The first two signals from the top correspond to electrodes located on the mother's thoracic region, and the last three signals correspond to

<sup>14</sup> <http://physionet.org/pn3/nifecgdb/>

electrodes located on the woman's abdomen. The recordings have been pre-processed: the baseline was eliminated using a low-pass filter with cutoff frequency equal to 0.7 Hz, and the powerline interference was attenuated using a notch filter.

Fig. 6 shows the source signals estimated by the same ICA algorithms used in the previous example (JADE, FastICA, FFD, SOBI and  $\pi$ CA). Only the maternal source signals can be recognized. We must conclude that, even though ICA is generally reliable, it sometimes fail.

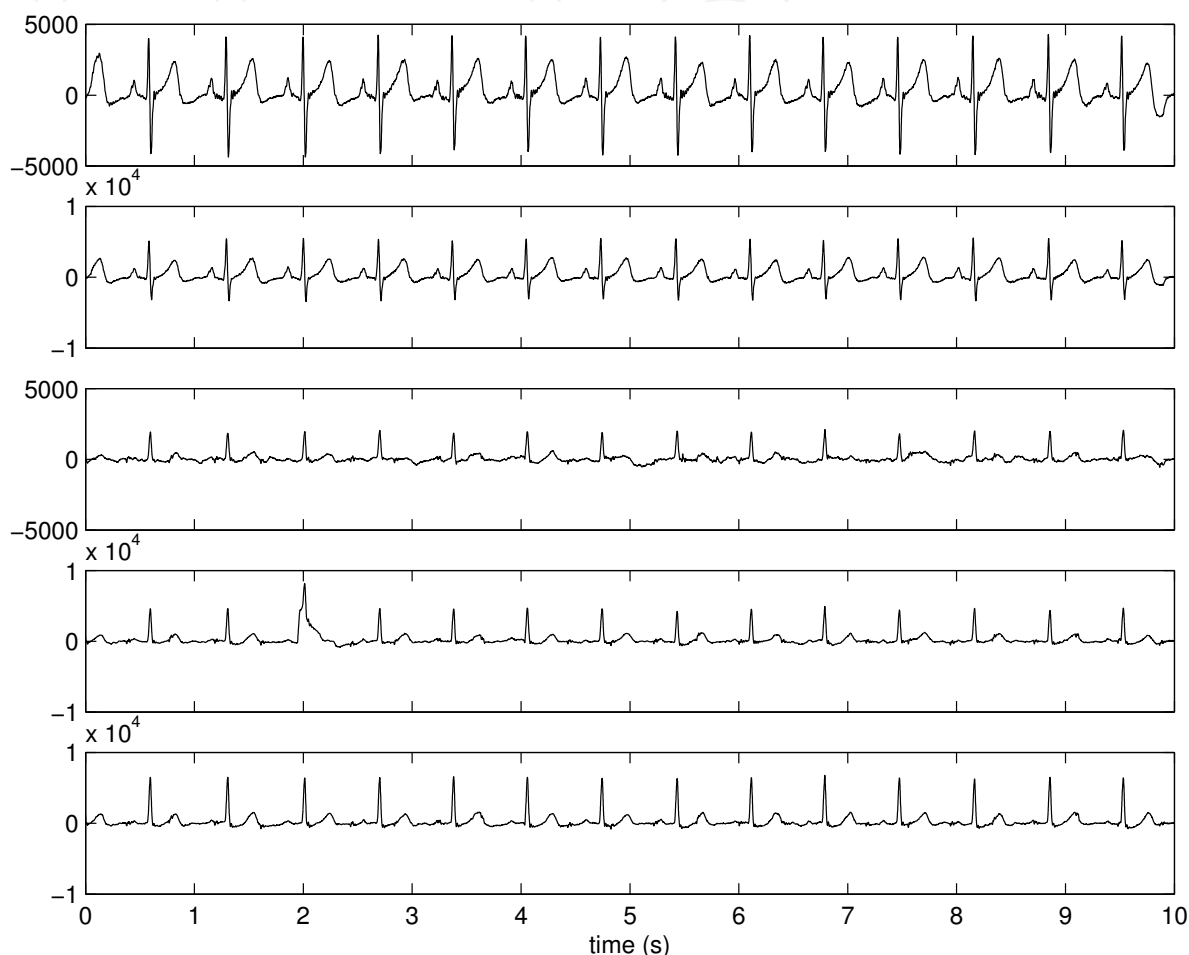


Fig. 5. Cutaneous electrode recordings from a pregnant woman in the 21 week of gestation.

### 7.3 Third example

We now repeat the previous (failed) experiment using the mECG as reference for the FFD method, as explained in Section 6. FFD has been chosen as representative of the ICA methods, but results are similar when any other of the algorithms is used. The estimated source signals are depicted in Fig. 7. Unlike in the previous experiment, the fECG is visible in the third plot from the top, and the fetal heart rate can be estimated even though the signal-to-noise ratio is low. Further denoising may necessary using other techniques –see, e.g., Sameni, Shamsollahi, Jutten & Clifford (2007); Vigneron et al. (2003)– but this is beyond the scope of the present Chapter.



Fig. 6. Source signals estimated by the different algorithms from the recordings of Fig. 5.

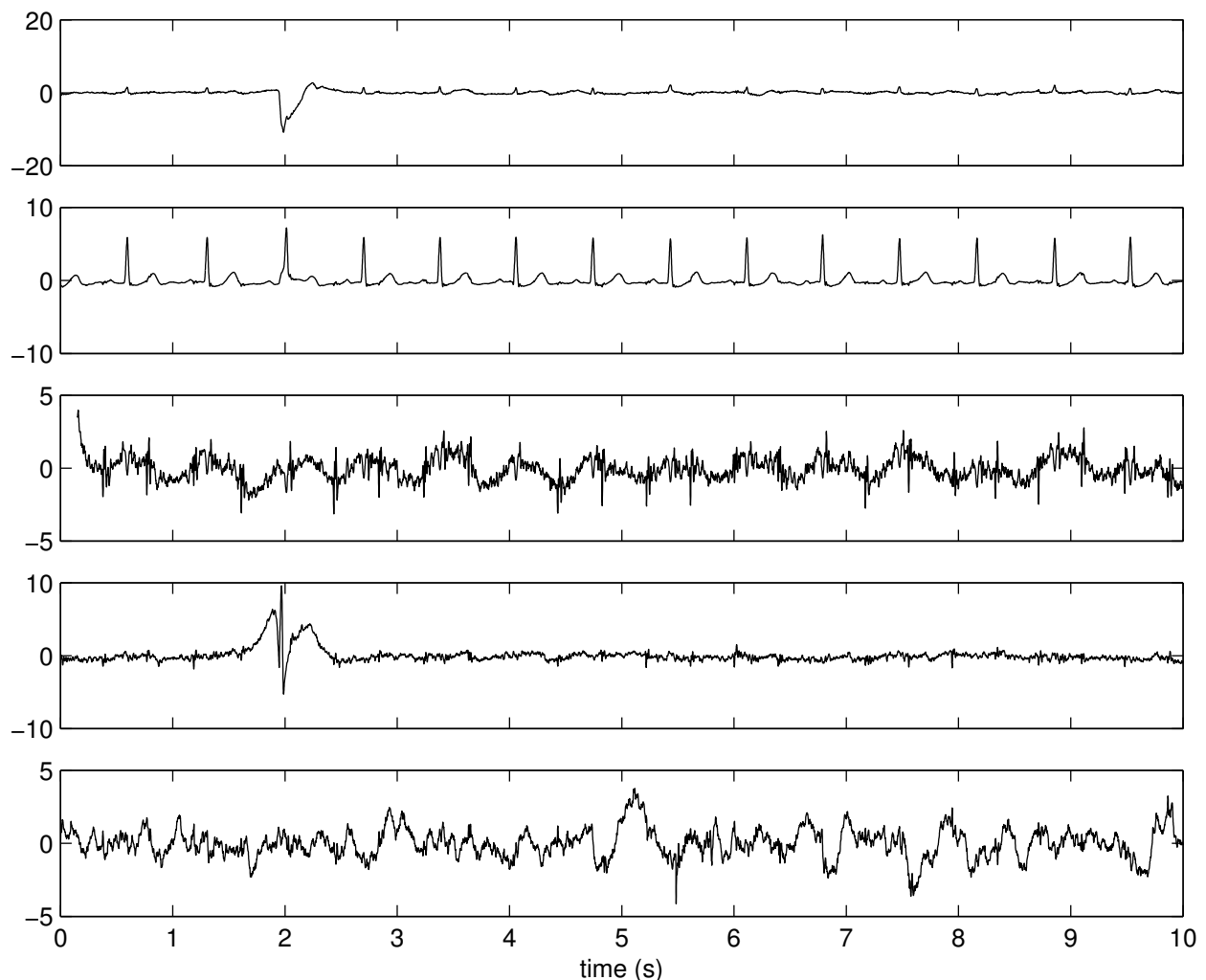


Fig. 7. Source signals detected from the recordings of Fig. 5 by using the mECG as reference.

## 8. Conclusions

This Chapter has presented a review of the state-of-the-art in the use of ICA for the fECG detection problem. A significant improvement in technical support for fetal monitoring has been obtained in the last decades. Compared to alternative techniques (e.g., filtering, average beat subtraction ...), ICA has proven to be a powerful and leading-edge approach. The most remarkable feature of higher-order ICA methods is that they do not seem to be very sensitive to the location of the electrodes. However, it should be pointed out that, even though promising results have been obtained (the fetal heart rate can be almost routinely determined), there is at present a total lack of accuracy in the detection of the smallest waves (P, Q, S and T) of the fECG. Though it is true that in current clinical practice the physician only considers the fetal cardiac rate, further research is therefore needed to improve accuracy of wave detection. The use of prior information (e.g., reference signals, or the knowledge about the fECG waveform) may be the strategy to achieve this goal. The physical interpretation of the estimated source signals also seems to be an exciting field for future work, and the independence of the sources need to be elucidated.

## 9. Acknowledgement

This work was supported by a grant from the “Junta de Andalucía” (Spain) with reference P07-TIC-02865.

## 10. References

- Abboud, S. & Sadeh, D. (1989). Spectral analysis of the fetal electrocardiogram, *Computers in biology and medicine* 19(6): 409–415.
- Abuhamad, A. & Chaoui, R. (2009). *A Practical Guide to Fetal Echocardiography: Normal and Abnormal Hearts*, Lippincott Williams & Wilkins.
- Adib, A. & Aboutajdine, D. (2005). Reference-based blind source separation using a deflation approach, *Signal Processing* 85: 1943 – 1949.
- Afriat, C. & Kopel, E. (2008). *Electronic Fetal Monitoring*, 2nd. edn, Lippincott Williams & Wilkins.
- Azzerboni, B., La Foresta, F., Mammone, N. & Morabito, F. (2005). A new approach based on wavelet-ica algorithms for fetal electrocardiogram extraction, *Proceeding of European symposium on Artificial Neural Networks*.
- Bai, Z., Demmel, J., Dongarra, J., Ruhe, A. & van der Vorst, H. (eds) (2000). *Templates for the Solution of Algebraic Eigenvalue Problems: A Practical Guide.*, SIAM.
- Barros, A. & Cichocki, A. (2001). Extraction of specific signals with temporal structure, *Neural Computation* 13(9): 1995–2003.
- Bell, A. J. & Sejnowski, T. (1995). An information-maximization approach to blind separation and blind deconvolution, *Neural Computation* 7: 1129–1159.
- Belouchrani, A., Abed-Meraim, K., Cardoso, J. & Moulines, E. (1997). A blind source separation technique using second-order statistics, *Signal Processing, IEEE Transactions on* 45(2): 434–444.
- Callaerts, D., Moor, B. D., Vandewalle, J. & Sansen, W. (1990). Comparison of svd methods to extract the foetal ecg from cutaneous electrode signals, *Medical & Biolog. Eng. & Computing* 28: 217–224.
- Camargo-Olivares, J., Martín-Clemente, R., Hornillo, S., Elena-Pérez, M. & Román-Martínez, I. (2011). The maternal abdominal ecg as input to mica in the fetal ecg extraction problem., *IEEE Signal Processing Letters* 18(3): 161 –164.
- Cardoso, J. F. (1998). Multidimensional independent component analysis, *Proc. ICASSP'98, Seattle*, pp. 1941–1944.
- Cardoso, J. F. & Souloumiac, A. (1993). Blind beamforming for non gaussian signals, *IEE Proceedings - F* 140(6): 363 – 370.
- Castells, F., Cebrián, A. & Millet, J. (2007). The role of independent component analysis in the signal processing of ecg recordings, *Biomedizinische Technik* 52(1): 18 – 24.
- Chan, A. (2008). *Biomedical device technology: principles and design*, Charles C. Thomas.
- Cichocki, A. & Amari, S.-I. (2002). *Adaptive blind signal and image processing: learning algorithms and applications*, Wiley.
- Cicinelli, E., Bortone, A., Carbonara, I., Incampo, G., Bochicchio, M., Ventura, G., Montanaro, S. & Aloisio, G. (1994). Improved equipment for abdominal fetal electrocardiogram recording: description and clinical evaluation, *International journal of bio-medical computing* 35(3): 193 – 205.
- Clifford, G., Sameni, R., Ward, J., Robinson, J. & Wolfberg, A. J. (2011). Clinically accurate fetal ecg parameters acquired from maternal abdominal sensors, *American Journal of Obstetrics and Gynecology* 205 (1): 47.e1–47.e5.

- Clifford, G., Shoeb, A., McSharry, P. & Janz, B. (2005). Model-based filtering, compression and classification of the ecg, *Proceedings of Bioelectromagnetism and 5th International Symposium on Noninvasive Functional Source Imaging within the Human Brain and Heart (BEM & NFSI)*.
- Comon, P. (1994). Independent component analysis, a new concept?, *Signal Processing (Special Issue Higher-Order Statistics)* 36 (3): 287–314.
- Comon, P. & Jutten, C. (eds) (2010). *Handbook of blind source separation, independent component analysis and applications*, Elsevier.
- De Lathauwer, L., Callaerts, D., De Moor, B. D. & Vandewalle, J. (1995). Fetal electrocardiogram extraction by source subspace separation, *Proc. IEEE SP/ATHOS Workshop on HOS*, Girona, Spain, pp. 134–138.
- De Lathauwer, L., De Moor, B. D. & Vandewalle, J. (2000a). Fetal electrocardiogram extraction by blind source subspace separation, *IEEE Transactions on Biomedical Engineering* 47 (5): 567–572.
- De Lathauwer, L., De Moor, B. & Vandewalle, J. (2000b). Svd-based methodologies for fetal electrocardiogram extraction, *Proceedings of the 2000 IEEE Int. Conf. on Acoustics, Speech, and Signal Processing (ICASSP'00)*, Vol. 6, pp. 3771 – 3774.
- Devedeux, D., Marque, C., Mansour, S., Germain, G., Duchêne, J. et al. (1993). Uterine electromyography: a critical review., *American journal of obstetrics and gynecology* 169(6): 1636 –1652.
- Freeman, R. & Garite, T. (2003). *Fetal Heart Rate Monitoring*, Lippincott Williams & Wilkins.
- Gao, P., Chang, E. & Wyse, L. (2003). Blind separation of fetal ecg from single mixture using svd and ica, *Information, Communications and Signal Processing, 2003 and the Fourth Pacific Rim Conference on Multimedia. Proceedings of the 2003 Joint Conference of the Fourth International Conference on*, Vol. 3, IEEE, pp. 1418–1422.
- Guyton, A. & Hall, J. (1996). *Textbook of Medical Physiology*, W. B. Saunders Company.
- Hasan, M., Reaz, M., Ibrahimy, M., Hussain, M. & Uddin, J. (2009). Detection and processing techniques of fecg signal for fetal monitoring, *Biological procedures online* 11(1): 263 – 295.
- Hyvärinen, A. (1999). Fast and robust fixed-point algorithms for independent component analysis, *IEEE Transactions on Neural Networks* 10 (3): 626–634.
- Hyvärinen, A., Karhunen, J. & Oja, E. (2001). *Independent Component Analysis*, John Wiley & Sons.
- James, C. & Hesse, C. (2005). Independent component analysis for biomedical signals, *Physiological measurement* 26: R15.
- Jenkins, H. M. L., Symonds, E. M., Kirk, D. L. & Smith, P. R. (2005). Can fetal electrocardiography improve the prediction of intrapartum fetal acidosis?, *BJOG: An International Journal of Obstetrics & Gynaecology* 93(1): 6–12.
- Kanjilal, P., Palit, S. & Saha, G. (1997). Fetal ecg extraction from single-channel maternal ecg using singular value decomposition, *IEEE Tr. on Biomedical Engineering* 44 (1): 51 – 59.
- Karvanen, J., Eriksson, J. & Koivunen, V. (2000). Pearson system based method for blind separation, *Proceedings of Second International Workshop on Independent Component Analysis and Blind Signal Separation (ICA2000)*, Helsinki, Finland, pp. 585–590.
- Keener, J. & Sneyd, J. (2009). *Mathematical Physiology*, Vol. 2, Springer.
- Keralapura, M., Pourfathi, M. & Sirkeci-Mergen, B. (2011). Impact of contrast functions in fast-ica on twin ecg separation, *IAENG International Journal of Computer Science* 38:1.
- Lewis, M. (2003). Review of electromagnetic source investigations of the fetal heart., *Medical Engineering and Physics* 25 (10): 801 – 810.

- Li, Y. & Yi, Z. (2008). An algorithm for extracting fetal electrocardiogram, *Neurocomputing* 71(7–9): 1538 – 1542.
- Llinares, R. & Igual, J. (2009). Application of constrained independent component analysis algorithms in electrocardiogram arrhythmias, *Artificial Intelligence in Medicine* 47: 121–133.
- Marossero, D., Erdogmus, D., Euliano, N., Principe, J., Hild, K. et al. (2003). Independent components analysis for fetal electrocardiogram extraction: a case for the data efficient mermaid algorithm, *Neural Networks for Signal Processing, 2003. NNSP'03. 2003 IEEE 13th Workshop on, IEEE*, pp. 399–408.
- Martín-Clemente, R., Acha, J. & Puntonet, C. G. (2004). Eigendecomposition of self-tuned cumulant-matrices for blind source separation, *Signal Processing* 84(7): 1201 – 1211.
- Martín-Clemente, R., Camargo-Olivares, J., Hornillo-Mellado, S., Elena, M. & Roman, I. (2011). Fast technique for noninvasive fetal ecg extraction, *IEEE Transactions on Biomedical Engineering* 58(2): 227 – 230.
- McSharry, P., G., C., Tarassenko, L. & Smith, L. (2003). A dynamical model for generating synthetic electrocardiogram signals, *IEEE Tr. on Biomedical Engineering* 50 (3): 289–294.
- Nait-Ali, A. (2009). *Advanced Biosignal Processing*, Springer Verlag.
- Oldenburg, J. & Macklin, M. (1977). Changes in the conduction of the fetal electrocardiogram to the maternal abdominal surface during gestation., *American journal of obstetrics and gynecology* 129(4): 425 – 433.
- Oostendorp, T. F. (1989). Lead systems for the abdominal fetal electrocardiogram, *Clinical Physics and Physiological Measurements* 10(21): 21 – 26.
- Oostendorp, T. F., van Oosterom, A. & Jongsma, H. W. (1989a). The effect of changes in the conductive medium on the fetal ecg throughout gestation, *Clinical Physics and Physiological Measurements* 10 (B): 11 – 20.
- Oostendorp, T. F., van Oosterom, A. & Jongsma, H. W. (1989b). The fetal ecg throughout the second half of gestation, *Clinical Physics and Physiological Measurements* 10 (2): 147 – 160.
- Pardi, G., Ferrazzi, E., Cetin, I., Rampello, S., Baselli, G., Cerutti, S., Civardi, S. et al. (1986). The clinical relevance of the abdominal fetal electrocardiogram., *Journal of perinatal medicine* 14(6): 371 – 377.
- Peters, M., Stinstra, J., Uzunbajakau, S. & Srinivasan, N. (2005). *Advances in electromagnetic fields in living systems*, Springer Verlag, chapter Fetal Magnetocardiography, pp. 1 – 40.
- Rieta, J., Castells, F., Sánchez, C., Zarzoso, V. & Millet, J. (2004). Atrial activity extraction for atrial fibrillation analysis using blind source separation, *IEEE Transactions on Biomedical Engineering* 51(7): 1176 – 1186.
- Sameni, R., Clifford, G., Jutten, C. & Shamsollahi, M. (2007). Multichannel ecg and noise modeling: Application to maternal and fetal ecg signals, *EURASIP Journal on Advances in Signal Processing* 2007.
- Sameni, R., Jutten, C. & M. Shamsollahi, M. (2006). What ica provides for ecg processing: application to non-invasive fetal ecg extraction, *Proc. 2006 IEEE International Symposium on Signal Processing and Information Technology*.
- Sameni, R., Jutten, C. & Shamsollahi, M. (2008). Multichannel electrocardiogram decomposition using periodic component analysis, *IEEE Transactions on Biomedical Engineering* 55 (8): 1935 – 1940.
- Sameni, R., Shamsollahi, M., Jutten, C. & Clifford, G. (2007). A nonlinear bayesian filtering framework for ecg denoising, *IEEE Tr. on Biomedical Engineering* 54(12): 2172 – 2185.

- Saul, L. K. & Allen, J. B. (2001). *Advances in Neural Information Processing Systems 13*, MIT Press: Cambridge, MA, chapter Periodic component analysis: an eigenvalue method for representing periodic structure in speech., pp. 807 – 813.
- Symonds, E. M., Sahota, D. & Chang, A. (2001). *Fetal Electrocardiography*, Imperial College Press.
- Tanskanen, J. & Viik, J. (2012). *Advances in Electrocardiograms - Methods and Analysis*, InTech, chapter Independent Component Analysis in ECG Signal Processing, pp. 349 – 372.
- Taylor, M., Smith, M., Thomas, M., Green, A., Cheng, F., Oseku-Afful, S., Wee, L., Fisk, N. & Gardiner, H. (2003). Non-invasive fetal electrocardiography in singleton and multiple pregnancies, *BJOG: An International Journal of Obstetrics & Gynaecology* 110(7): 668 – 678.
- Taylor, M., Thomas, M., Smith, M., Oseku, S., Fisk, N., Green, A., Paterson, S. & Gardiner, H. (2005). Non-invasive intrapartum fetal ecg: preliminary report., *Br. J. Obstet. Gynaecol.* 112: 1016–1021.
- Theis, F. J. (2004). Uniqueness of complex and multidimensional independent component analysis., *Signal Processing* 84 (5): 951–956.
- Tong, L., Liu, R., Soon, V. C. & Huang, Y.-F. (1991). Indeterminacy and identifiability of blind identification, *IEEE Transactions on Circuit and Systems* 38 (5): 499 – 509.
- Tsalaile, T., Sameni, R., Sanei, S., Jutten, C. & Chambers, J. (2009). Sequential blind source extraction for quasi-periodic signals with time-varying period, *IEEE Tr. on Biomedical Engineering* 56(3): 654 – 655.
- Vetter, R., Virag, N., Vesin, J., Celka, P. & Scherrer, U. (2000). Observer of autonomic cardiac outflow based on blind source separation of ecg parameters, *IEEE Transactions on Biomedical Engineering* 47: 589–593.
- Vigeneron, V., Paraschiv-Ionescu, A., Azancot, A., Sibony, O. & Jutten, C. (2003). Fetal electrocardiogram extraction based on non-stationary ica and wavelet denoising, *Signal Processing and Its Applications, 2003. Proceedings. Seventh International Symposium on*, Vol. 2, pp. 69 – 72.
- Vollgraf, R. & Obermayer, K. (2001). Multi-dimensional ica to separate correlated sources., *Proceeding of Neural Information Processing System (NIPS)*, pp. 993–1000.
- Vrins, F., Jutten, C. & Verleysen, M. (2004). Sensor array and electrode selection for non-invasive fetal electrocardiogram extraction by independent component analysis, *Independent Component Analysis and Blind Signal Separation* pp. 1017–1024.
- Wakai, R., Lengle, J. & Leuthold, A. (2000). Transmission of electric and magnetic foetal cardiac signals in a case of ectopia cordis: the dominant role of the vernix caseosa, *Physics in medicine and biology* 45: 1989 – 1995.
- Yu, S. & Chou, K. (2008). Integration of independent component analysis and neural networks for ecg beat classification, *Expert Systems with Applications* 34(4): 2841–2846.
- Zarzoso, V. (2009). *Advanced Biosignal Processing*, Springer, chapter Extraction of ECG Characteristics Using Source Separation Techniques: Exploiting Statistical Independence and Beyond.
- Zarzoso, V. & Nandi, A. K. (2001). Noninvasive fetal electrocardiogram extraction: blind separation versus adaptive noise cancelation., *IEEE Tr. on Biomedical Engineering* 48 (1): 12–18.

© 2012 The Author(s). Licensee IntechOpen. This is an open access article distributed under the terms of the [Creative Commons Attribution 3.0 License](#), which permits unrestricted use, distribution, and reproduction in any medium, provided the original work is properly cited.

IntechOpen

IntechOpen